ORGANIC CHEMISTRY FRONTIERS

RESEARCH ARTICLE

View Article Online
View Journal | View Issue

Cite this: *Org. Chem. Front.*, 2023, **10**, 3193

Galvinoxyl-inspired dinitronyl nitroxide: structural, magnetic, and theoretical studies†

Takuya Kanetomo, * Sayaka Ono, Yusuke Fukushima, Yuta Takenouchi and Masaya Enomoto *

Received 21st April 2023,
Accepted 12th May 2023

DOI: 10.1039/d3qo00591g

rsc.li/frontiers-organic

A novel galvinoxyl-inspired dinitronyl nitroxide (**1**) has been synthesized. Structural analysis revealed that **1** exhibited a resonance structure, resulting from *p*-benzoquinonediimine *N*,*N*′-dioxide and *N*-phenyl nitroxide moieties. The magnetic study revealed an intramolecular exchange-coupling constant J/k_B of −761 (3) K in $H = -J(S_1 \cdot S_2 + S_2 \cdot S_3)$, indicating a ground doublet state. Theoretical calculations suggested not only the strong intramolecular antiferromagnetic coupling but also a unique electron configuration owing to a remarkable spin polarization effect.

Introduction

Organic radicals have many uses in the fields of spin trapping,[1,2] spin labeling,[3,4] dynamic nuclear polarization,[5,6] organic catalysts,[7,8] photochromic materials,[9,10] and molecular magnetic materials.[11–16] An understanding of not only the physical properties but also the chemical stability of these unique radical-based materials is required. There are two approaches to stabilize radical species: (i) delocalization of the radical spin on the π-conjugated system and (ii) steric protection around the radical centre with bulky substituents.[17]

Galvinoxyl reported by Coppinger is well known as a stable radical (Fig. 1a).[18] The unpaired electron is delocalized throughout the molecule, and the *tert*-butyl groups play a role in steric protection. These factors impart both thermodynamic and kinetic stabilities to the molecule. As shown in Fig. 1a, galvinoxyl can be illustrated as a triradical, but it behaves as a monoradical species due to strong intramolecular antiferromagnetic coupling. Such triradicals with a doublet ground state ($S = 1/2$) have been reported several times.[19–22] Interestingly, galvinoxyl exhibits a difference in the spin polarization of the α and β spins owing to the strong intramolecular antiferromagnetic coupling; namely, the β-HOMO level is elevated to the α-SOMO level, where the SOMO and HOMO represent singly and doubly highest occupied molecular orbitals, respectively.[23,24] This electron configuration is known as a partial SOMO–HOMO inversion (SHI),[24] as shown in Fig. 1b. Owing to the thermal stability and the unique electron structure, several galvinoxyl analogues have been reported where the chemical modification is mainly at the methine position.[25–36]

In this study, we have synthesized a galvinoxyl-inspired dinitronyl nitroxide, 2,7-bis(*N*-*tert*-butyl-*N*-oxylamino)-10′-methyl-9,9′(10*H*,10′*H*)spirobiacridin-10-oxyl (**1**). The *N*-oxy-acridine side of **1** is an isoelectronic structure with galvinoxyl (Fig. 1c); namely, two oxygen and methine sites in galvinoxyl are replaced by nitroxides/nitrones. The NO site is more thermodynamically stable than phenoxy (>C–O•) due to a local

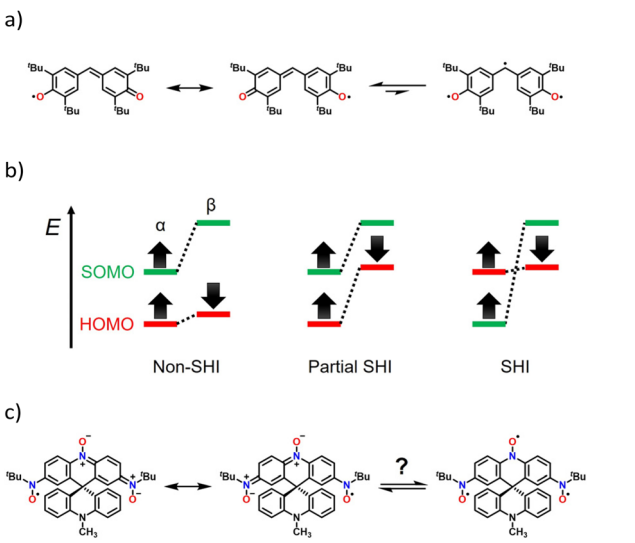

Fig. 1 Resonance and equilibrium schemes of (a) galvinoxyl and (c) dinitronyl nitroxide **1**. (b) Illustration for three electronic configurations, non-SHI, partial SHI, and SHI.

Department of Chemistry, Faculty of Science Division 1, Tokyo University of Science, 1-3 Kagurazaka, Shinjuku-ku, Tokyo, 162-8603, Japan.
E-mail: kanetomo@rs.tus.ac.jp

†Electronic supplementary information (ESI) available. CCDC 2256749. For ESI and crystallographic data in CIF or other electronic format see DOI: https://doi.org/10.1039/d3qo00591g

resonance structure of the >N–O$^{\bullet}$ and >N$^{\bullet+}$–O^{-} forms. This allows the removal of the *tert*-butyl substituents used in galvinoxyl, and a six-membered ring can be created in the central moiety. The latter improves the planarity of the whole molecule, resulting in strong intramolecular antiferromagnetic coupling. For **1**, the formation of the spiro structure with *N*-methyl-9(10*H*)acridine not only forms the central six-membered ring but also introduces steric protection. According to Iwamura's work, the 1,4-phenylene bisnitroxide moiety could be stabilized as a quinoid form, *p*-benzoquinonediimine *N*,*N*′-dioxide.[37] Therefore, **1** should favour the dinitronyl nitroxide monoradical structure (the left side in Fig. 1c). In fact, magnetic and theoretical studies of **1** exhibited the ground doublet state (S = 1/2). The MO diagram exhibited the partial SHI state as well as galvinoxyl, owing to the remarkable spin polarization effect.

Results and discussion

Synthesis and characterization

Compound **1** was synthesized by following the procedure shown in Scheme S1.† Black platelet polycrystals of **1** were obtained by recrystallization from CH_2Cl_2 and *n*-hexane. Product **1** was characterized through spectroscopic and X-ray crystallographic analyses. The decomposition temperature of **1** was 168 °C, where the thermal stability of **1** is similar to that of galvinoxyl (153 °C).[18]

The X-band electron spin resonance (ESR) spectrum of **1** in a toluene solution at room temperature (rt) is shown as a red line in Fig. 2. The spectrum was a major triplet splitting with several minor ones, indicating the hyperfine structures for one ^{14}N and three ^{1}H atoms. This pattern indicates that **1** in solution exhibits dinitronyl nitroxide as shown in Fig. 1c. It was also found that the radical spin could be localized in one benzenoid moiety. This finding is also reported in the study of galvinoxyl.[26,38,39] When bulky substituents such as *tert*-butyl or 1-adamantyl are introduced at the methine site of galvinoxyl, two phenyl rings are twisted, resulting in the unpaired electron being confined to one phenoxy ring. By means of simulation using the EasySpin software,[40] the hyperfine constants, g values, and the linewidth of peak-to-peak (lwpp) were determined as a_N = 1.17 mT, a_{H1} = 0.252 mT, a_{H2} = 0.182 mT, a_{H3} = 0.087 mT, g_{xx} = 2.0037, g_{yy} = 2.0069, g_{zz} = 2.0096, and lwpp = 0.164 mT. The simulation spectrum (a black line in Fig. 2), derived from the above parameters, well reproduced the experimental one. For **1**, two N–O sites could be twisted along a single bond relative to the acridine ring, leading to a situation similar to that of the galvinoxyl derivative with bulky substituents.

Time-dependent ESR measurements were performed under ambient conditions to assess the stability of **1** in solution (Fig. S1a†). The time dependence of the maximum intensities in the central peak is shown in Fig. S1b.† Fitting of the data shows an exponential decay of the ESR intensity, but the intensities did not reach zero for the measurement times. The hyperfine structure (a_H) gradually disappeared, resulting in a simplified triplet splitting pattern. This finding can be attributed to the infiltration of O_2 into the solution during storage.

Single-crystal X-ray crystallography

The crystal structure of **1** was evaluated at 93 K, and it crystallized in a monoclinic $P\bar{1}$ space group (Table S1†). There were two crystallographically independent molecules in a unit cell (Fig. 3a). Two independent molecules (**1a** and **1b**) are represented in Fig. 3b and c, respectively. There were disordered CH_2Cl_2 crystal solvents, which were accounted for in the SQUEEZE/PLATON program, and the electron count was 72 electrons per formula unit. This value is close to the 1.7 CH_2Cl_2 solvents (71 electrons). The N1–O1, N2–O2, and N3–O3

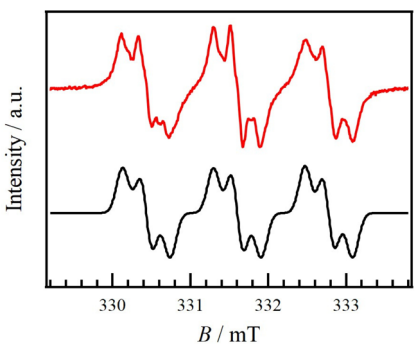

Fig. 2 X-Band ESR spectrum of **1** in a degassed toluene solution at 298 K. The top and bottom spectra represent the experimental and simulation, respectively. For the optimized parameters in the simulation, see the text.

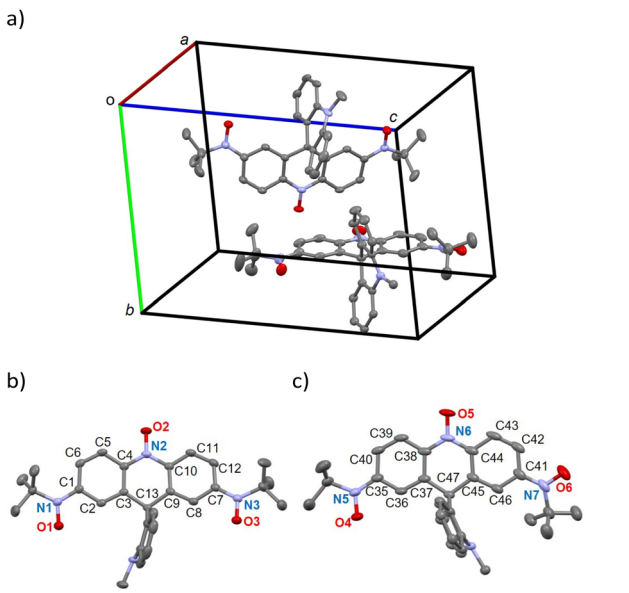

Fig. 3 Crystal structures of (a) asymmetry units in the unit cell and molecular structures of (b) **1a** and (c) **1b**. Thermal ellipsoids for non-hydrogen atoms are drawn at the 50% probability level. The H atoms and solvent molecules are omitted for clarity.

bond lengths of **1a** are 1.285(2), 1.295(2), and 1.281(2) Å, respectively, and the N5–O4, N6–O5, and N7–O6 bond lengths of **1b** are 1.285(3), 1.287(3), and 1.284(2) Å, respectively. These bond lengths are shorter than the average of about 1.45 Å for hydroxylamine compounds,[41–47] indicating successful oxidation. Three N–O sites in **1** show either nitroxides or nitrones, as shown in Fig. 1b. However, since both nitrones and nitroxides have an N–O length of about 1.3 Å,[16,19,37,48–85] the bond length between the N and neighbouring sp^2 carbon atoms is important to determine the electron state of the N–O site. In fact, there is a difference in the N–C_{sp^2} length; the average lengths for nitrones are 1.31 Å (N–O: 1.29 Å),[48–53] those for aryl *tert*-butyl nitroxides are 1.43 Å (N–O: 1.29 Å),[16,19,37,45,54–71] and those for 10-oxy-9(10*H*)acridines are 1.41 Å (N–O: 1.29 Å).[72–75] The compound 4,4,5,5-tetramethylimidazoline-3-oxide-1-oxyl, known as nitronyl nitroxide, has both nitrone and nitroxide moieties and thus an N–C_{sp^2} length of 1.34 Å (N–O: 1.28 Å),[41,54,55,76–85] which is intermediate between those of nitrone and nitroxide species. For **1a** and **1b**, the N–C_{sp^2} lengths are 1.380(3)–1.387(3) and 1.373(3)–1.396(4) Å, respectively. These values are close to those of nitronyl nitroxides, indicating a dinitronyl nitroxide structure (the left-side structures in Fig. 1b).

Dinitronyl nitroxide **1** possesses benzenoid and quinoid substructures, and the quinoid one shows bond alternation and reduction of aromaticity. In fact, 1,4-phenylene bis(*tert*-butyl nitroxide) (**2**) shows alternating C–C bond lengths (Table 1).[37] On the other hand, chemical modifications shifted the equilibrium in favour of the benzenoid form due to (i) linker elongation and (ii) steric hindrance. For example, the former are 4,4′-biphenyl- and 4,4″-1,1′:4′,1″-terphenylene bis(*tert*-butyl nitroxide) compounds (**3** and **4**, respectively),[86] and the latter is 2,3,5,6-tetramethoxy-1,4-phenylene bis(*tert*-butyl nitroxide) (**5**).[37] Selected bond lengths and torsion angles of **1a** and **1b** are summarized in Table 1. For comparison purpose, the data of **2**–**5** are also listed. A harmonic oscillator model for aromaticity (HOMA) value is useful for clarifying comparisons of bond lengths.[87,88] Four phenyl rings, C1–C6 (A) and C7–C12 (B) for **1a** and C35–C40 (C) and C41–C46 (D) for **1b**, show HOMA values of 0.844, 0.853, 0.806, and 0.922, respectively. For **1a**, the values are intermediate between those of the quinoid form **2** and the benzenoid forms **3**–**5**, indicating the delocalized radical spin throughout the acridine moiety. On the other hand, the HOMA values of the C and D rings in **1b** are smaller and larger, respectively, compared to **1a**. This finding implies that the C and D rings favour the quinoid and benzenoid forms, respectively. This situation is also supported by the large torsion angle between the D ring and the N–O site.

The nearest intermolecular NO···NO distance is 3.943(2) Å of O2···O2[a]. This value is larger than the sum of the van der Waals radii of O/O of 3.04 Å,[89] indicating no direct radical–radical contact. On the other hand, three O atoms, O2, O5[b], and O6[c], face each other around the C5 atom, as shown in Fig. S2.† The O2···O5, O5···O6, and O6···O2 distances of 4.007(3), 4.055(3), and 4.330(2) Å, respectively, are larger than the sum of vdW radii (O/O; 3.04 Å), while the O2···C5, O5···C5, and O6···C5 distances of 2.700(2), 3.058(3), and 3.237(2) Å, respectively, are smaller than it (C/O; 3.22 Å). These contacts between three O atoms through an H atom on the C5 atom could induce magnetic interaction.

Magnetic properties

Magnetic susceptibility was measured for the polycrystal sample **1** at 2–350 K (Fig. 4a). Note that the molecular weight is calculated excluding the crystalline solvent because the exact amount of solvent cannot be calculated due to the gradual desorption of the solvent during storage. Upon cooling from 350 K, the $\chi_m T$ value gradually decreased to a plateau at 100–10 K. This antiferromagnetic behaviour implies a depopulation from the quartet excited state (S = 3/2) to the doublet ground state (S = 1/2). On the other hand, the plateau value of about 0.32 cm^3 K mol^{-1} was smaller than the calculated $\chi_m T$ value of 0.378 cm^3 K mol^{-1} derived from S = 1/2 and g = 2.0067, where the g value is from the ESR study. This difference implies the presence of the residual crystal solvents in

Table 1 Selected structural parameters and HOMA values for **1a**, **1b**, and **2**–**5**

	1a		**1b**		**2** (n = 1)[a,b]		**3** (n = 2)[c]	**4** (n = 3)[c]	**5**[b]
	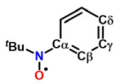		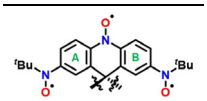		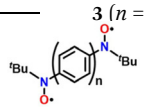				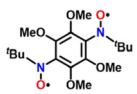
	A	B	C	D	*a*	*b*			
O–N/Å	1.285(2)	1.281(2)	1.285(3)	1.284(2)	1.290(5)	1.287(6)	1.284(1)	1.291(1)	1.269(5)
N–C_α/Å	1.384(2)	1.380(3)	1.373(3)	1.386(4)	1.353(6)	1.362(7)	1.411(1)	1.413(2)	1.428(5)
C_α–C_β/Å	1.412(2)	1.413(3)	1.407(4)	1.411(4)	1.422(6)	1.417(6)	1.406(1)	1.404(2)	1.393(7)
C_β–C_γ/Å	1.367(3)	1.368(3)	1.364(3)	1.362(4)	1.360(7)	1.358(7)	1.380(1)	1.385(2)	1.397(5)
C_γ–C_δ/Å	1.411(2)	1.406(2)	1.416(3)	1.405(3)	1.424(6)	1.423(6)	1.416(1)	1.405(2)	1.384(6)
$\lvert\angle$O–N–C_α–$C_\beta\rvert$/°	7.4(3)	2.8(3)	6.4(3)	24.3(3)	1.2(6)	3.3(7)	7.3(1)	15.3(2)	84.5(5)
HOMA[d]	0.844	0.853	0.806	0.922	0.722	0.745	0.925	0.955	0.990

[a] Compound **2** has two crystallographically independent molecules in the unit cell (molecules *a* and *b*). [b] Ref. 37. [c] Ref. 86. [d] Ref. 87 and 88.

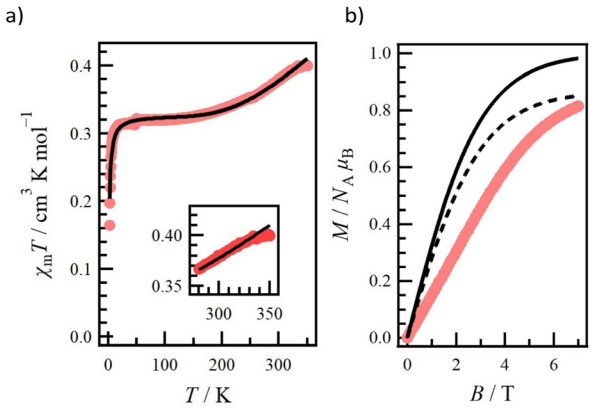

Fig. 4 (a) Temperature dependence of $\chi_m T$ for **1**, measured at B = 0.5 T. A solid line shows the fitting curve. The inset shows an enlarged view of the 280 to 350 K region. (b) M *vs.* B at 2.0 K. The solid line shows the Brillouin function with S = 1/2 and g = 2.0067. The dashed line is multiplied by 0.8668.

the sample. Upon further cooling from 10 K, the $\chi_m T$ value decreased sharply, indicating intermolecular antiferromagnetic coupling. The experimental data of **1** were analysed with eqn (1) based on the linear three S = 1/2 centre model, $\hat{H} = -J(\hat{S}_1 \cdot \hat{S}_2 + \hat{S}_2 \cdot \hat{S}_3)$.[90]

$$\chi_m T = \frac{N_A \mu_B{}^2 g^2}{4k_B} \frac{1 + \exp(J/k_B T) + 10\exp(3J/2k_B T)}{1 + \exp(J/k_B T) + 2\exp(3J/2k_B T)} \frac{T}{T - \theta} f \quad (1)$$

A Weiss mean-field parameter θ and a parameter f are introduced in order to estimate the intermolecular interaction in the low-temperature region and the amount of the residual CH_2Cl_2 as a crystal solvent, respectively. The g value was set at 2.0067. The best-fit curve was achieved with J/k_B = −761(3) K, θ = −1.22(3) K, and f = 0.8668(9) (a black line in Fig. 4a). The J value was negative, indicating the doublet ground state arising from the through-bond antiferromagnetic interaction, while the magnitude of J is discussed in the theoretical calculations below. The θ value was negative and small due to indirect contacts (Fig. S4†). From the f value of 0.8668(9), we estimated the amount of the CH_2Cl_2 crystal solvent required for the calculated molecular weight, resulting in 0.991 molecules. This value is less than the 1.7 molecules observed in the above structural study, suggesting desorption of the solvent during storage. Above 330 K, the experimental $\chi_m T$ deviated from the fitting line (the inset of Fig. 4a), and this may be triggered by the desorption of the residual crystal solvents.

The field-dependence of the magnetization curve at 2 K is shown in Fig. 4b. The M value was not saturated and reached 0.814μ_B at 7 T. Compared to the black solid line in Fig. 4b, which is derived from the Brillouin function with S = 1/2 and g = 2.0067, there is a difference in the scale of the experimental and simulation curves. Therefore, the black dashed line in Fig. 4b is drawn, considering the purity factor f = 0.8668. The magnitude of M in the simulation is well in agreement with the experimental curve, whereas the experimental curve is within the simulation. This result indicates an antiferromagnetic interaction, supporting the negative θ constant.

Theoretical studies

The density functional theory (DFT) calculations on **1a** and **1b** were performed using the atomic coordination determined from the crystallographic study. For reducing calculation cost, the *N*-methyl acridine ring and *tert*-butyl groups were replaced with H atoms and methyl groups, respectively. The calculated spin densities of the doublet (d) and quartet (q) states for **1a** and **1b** have been mapped onto the molecular skeleton shown in Fig. 5. There is a difference in the maps of the doublet state in **1a** and **1b**. For **1a**, the red and blue lobes, which represent positive and negative spin densities, appeared alternately along the π-conjugation system owing to the spin polarization (Fig. 5a). On the other hand, for **1b**, two-coloured lobes appeared alternately only on the left-hand six-membered ring, while on the right-hand one, the spin density is strongly localized at the N–O site. The quartet and doublet energy states for **1a** were E_q = −969.95114196 au with $\langle S^2 \rangle_q$ = 3.7501 and E_d = −969.97229443 au with $\langle S^2 \rangle_d$ = 0.8284, respectively. Those parameters for **1b** were E_q = −969.94969131 au with $\langle S^2 \rangle_q$ = 3.7501, and the E_d energy was −969.96185149 au with $\langle S^2 \rangle_d$ = 0.8112. The ΔE_{q-d} values of **1a** and **1b** were determined to be +0.5756 and +0.3309 eV, respectively. The exchange-coupling constant J/k_B values for **1a** and **1b** are also −1589 and −908 K, respectively, calculated by the approximate spin-projection method,[91] $J = (E_d - E_q)/(\langle S^2 \rangle_q - \langle S^2 \rangle_d)$. These findings indicate that both **1a** and **1b** show the ground doublet state.

The molecular orbitals (MOs) of the doublet state for **1a** and **1b** are shown in the left and right columns of Fig. 6, respectively. The α- and β-MO1–3 levels in **1a** and **1b** are obviously separated from the other MO levels, and thus these MOs play the key role in determining the spin state. For **1a**, α-MO2 and β-MO2 (−5.53 and −2.94 eV), α-MO1 and β-MO3 (−2.79 and −5.42 eV), and α-MO3 and β-MO1 (−5.77 and −2.42 eV) are paired, respectively, according to the comparison of

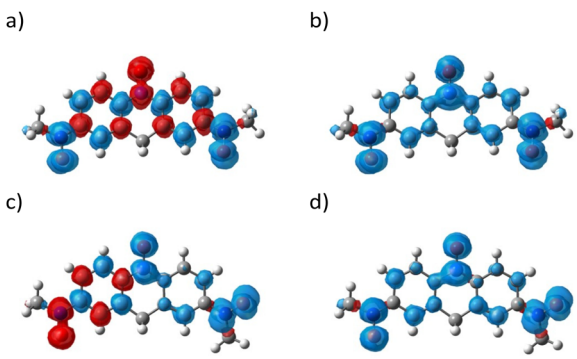

Fig. 5 Spin-density maps illustrating the DFT results for the (a) doublet and (b) quartet states of **1a** and the (c) doublet and (d) quartet states of **1b**. Those atomic positions were taken from the crystallographic study. Blue and red lobes indicate positive and negative spin densities, respectively, with the isocontour of 0.002 e Å^{-3}.

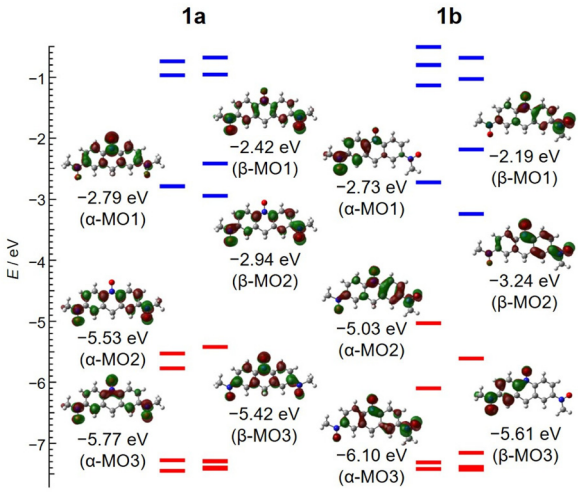

Fig. 6 Molecular-orbital (MO) energy-level diagram for α and β spins in the doublet state of (left) **1a** and (right) **1b** (isovalue = 0.03). Blue and red colours represent unoccupied and occupied orbitals, respectively. Selected MO images are superposed.

those MO maps shown in Fig. 6. The orbital lobes of β-MO3 are positioned to avoid those of α-MO2, reducing electron repulsion; namely, there is a remarkable effect of spin polarization. This situation implies intramolecular antiferromagnetic coupling between the terminal and central N–O sites, providing a partial SHI state like galvinoxyl. On the other hand, there is a difference in the MO diagram of **1b** and **1a**. According to the structural study, the unpaired electron of **1b** is localized on the N7–O6 site with the C42–C47 (D) ring. Those MO maps shown in Fig. 6 imply that α-MO1 and β-MO3 (−2.73 and −5.61 eV), α-MO2 and β-MO1 (−5.03 and −2.19 eV), and α-MO3 and β-MO2 (−6.10 and −3.24 eV) are paired. For the occupied MOs, α-MO2, α-MO1, and β-MO3, the arrangement of the molecular lobes on the left-side ring is affected by spin polarization, which is supported by the quinoid form observed in the structural study. However, only the α spin exists on the right-side ring. These results suggest that the radical spin is localized at the N–O site on the right-side ring. The differences in spin densities and MOs of **1a** and **1b** were caused by the degree of tilt of the N–O site to the acridine ring.

Conclusions

We have prepared the novel galvinoxyl-inspired dinitronyl nitroxide **1**, which shows a ground doublet state (S = 1/2) as confirmed by magnetic measurements. Compound **1a** shows high coplanarity between the acridine and N–O sites. The unpaired electron is delocalized throughout the acridine ring, resulting in thermodynamic stability similar to that of galvinoxyl. DFT calculations reveal strong intramolecular antiferromagnetic coupling and a remarkable spin polarization effect. On the other hand, in **1b**, one N–O site is twisted relative to the acridine ring, and the radical spin is localized to one phenyl ring. According to the ESR study, in solution, the radical spin localizes either on the phenyl rings due to the configuration of the N–O sites or the *N*-methyl acridine sites. Therefore, these studies on **1** reveal that the SOMO and HOMO electronic configurations are highly responsive to the conformation of the N–O sites. This highly responsive electronic structure makes it possible to produce a switching material that is triggered by the external environment.

Conflicts of interest

There are no conflicts to declare.

Acknowledgements

This study was financially supported by KAKENHI (JSPS, 20K22538). Prof. Takayuki Ishida (The University of Electro-Communications) kindly lent HPLC (Japan Analytical Industry, 1H + 1H GPC columns; a flow rate of 3.5 mL min^{-1}) for the isolation of **1**. The crystallography study for **1** was supported by "Advanced Research Infrastructure for Materials and Nanotechnology in Japan (ARIM)" of the Ministry of Education, Culture, Sports, Science and Technology (MEXT), Grant Number A-22-UT-0080.

References

1 E. G. Janzen, Spin trapping, *Acc. Chem. Res.*, 1971, **4**, 31–40.
2 M. J. Davies, Detection and characterisation of radicals using electron paramagnetic resonance (EPR) spin trapping and related methods, *Methods*, 2016, **109**, 21–30.
3 J. F. W. Keana, Newer aspects of the synthesis and chemistry of nitroxide spin labels, *Chem. Rev.*, 1978, **78**, 37–64.
4 A. Bonucci, O. Ouari, B. Guigliarelli, V. Belle and E. Mileo, In-Cell EPR: Progress towards Structural Studies Inside Cells, *ChemBioChem*, 2020, **21**, 451–460.
5 O. Haze, B. Corzilius, A. A. Smith, R. G. Griffin and T. M. Swager, Water-Soluble Narrow-Line Radicals for Dynamic Nuclear Polarization, *J. Am. Chem. Soc.*, 2012, **134**, 14287–14290.
6 D. Wisser, G. Karthikeyan, A. Lund, G. Casano, H. Karoui, M. Yulikov, G. Menzildjian, A. C. Pinon, A. Purea, F. Engelke, S. R. Chaudhari, D. Kubicki, A. J. Rossini, I. B. Moroz, D. Gajan, C. Copéret, G. Jeschke, M. Lelli, L. Emsley, A. Lesage and O. Ouari, *J. Am. Chem. Soc.*, 2018, **140**, 13340.
7 L. Li, R. Matsuda, I. Tanaka, H. Sato, P. Kanoo, H. J. Jeon, M. L. Foo, A. Wakamiya, Y. Murata and S. Kitagawa, A Crystalline Porous Coordination Polymer Decorated with Nitroxyl Radicals Catalyzes Aerobic Oxidation of Alcohols, *J. Am. Chem. Soc.*, 2014, **136**, 7543–7546.
8 P. Qu, M. Kuepfert, S. Jockusch and M. Weck, Compartmentalized Nanoreactors for One-Pot Redox-Driven Transformations, *ACS Catal.*, 2019, **9**, 2701–2706.

9 R. Dessauer, *Photochemistry, History, and Commercial Applications of Hexaarylbiimidazoles*, Elsevier, 2006.
10 A. Tokunaga, L. M. Uriarte, K. Mutoh, E. Fron, J. Hofkens, M. Sliwa and J. Abe, Photochromic Reaction by Red Light via Triplet Fusion Upconversion, *J. Am. Chem. Soc.*, 2019, **141**, 17744–17753.
11 I. Ratera and J. Veciana, Playing with organic radicals as building blocks for functional molecular materials, *Chem. Soc. Rev.*, 2012, **41**, 303–349.
12 N. M. Gallagher, A. Olankitwanit and A. Rajca, High-Spin Organic Molecules, *J. Org. Chem.*, 2015, **80**, 1291–1298.
13 E. Jin, M. Asada, Q. Xu, S. Dalapati, M. A. Addicoat, M. A. Brady, H. Xu, T. Nakamura, T. Heine, Q. Chen and D. Jiang, Two-dimensional sp^2 carbon–conjugated covalent organic frameworks, *Science*, 2017, **357**, 673–676.
14 N. Nakamura, K. Inoue, H. Iwamura, T. Fujioka and Y. Sawaki, Synthesis and characterization of a branched-chain hexacarbene in a tridecet ground state. An approach to superparamagnetic polycarbenes, *J. Am. Chem. Soc.*, 1992, **114**, 1484–1485.
15 A. Rajca and S. Utamapanya, Toward organic synthesis of a magnetic particle: dendritic polyradicals with 15 and 31 centers for unpaired electrons, *J. Am. Chem. Soc.*, 1993, **115**, 10688–10694.
16 J. Fujita, Y. Matsuoka, K. Matsuo, M. Tanaka, T. Akita, N. Koga and H. Iwamura, Molecular structure and magnetic properties of N,N-bis{4-methoxy-3,5-bis(N-tert-butyl-N-oxyamino)phenyl)}aminoxyl. An approach to a stable and high-spin pentaradical, *Chem. Commun.*, 1997, 2393–2394.
17 B. Tang, J. Zhao, J.-F. Xu and X. Zhang, Tuning the stability of organic radicals: from covalent approaches to non-covalent approaches, *Chem. Sci.*, 2020, **11**, 1192–1204.
18 G. M. Coppinger, A stable phenoxy radical inert to oxygen, *J. Am. Chem. Soc.*, 1957, **79**, 501–502.
19 S. Suzuki, A. Nagata, M. Kuratsu, M. Kozaki, R. Tanaka, D. Shiomi, K. Sugisaki, K. Toyota, K. Sato, T. Takui and K. Okada, Trinitroxide-Trioxytriphenylamine: Spin-State Conversion from Triradical Doublet to Diradical Cation Triplet by Oxidative Modulation of a π-Conjugated System, *Angew. Chem., Int. Ed.*, 2012, **51**, 3193–3197.
20 X. Lu, S. Lee, Y. Hong, H. Phan, T. Y. Gopalakrishna, T. S. Herng, T. Tanaka, M. E. Sandoval-Salinas, W. Zeng, J. Ding, D. Casanova, A. Osuka, D. Kim and J. Wu, Fluorenyl Based Macrocyclic Polyradicaloids, *J. Am. Chem. Soc.*, 2017, **139**, 13173–13183.
21 T. Kodama, M. Aoba, Y. Hirao, S. M. Rivero, J. Casado and T. Kubo, Molecular and Spin Structures of a Through-Space Conjugated Triradical System, *Angew. Chem., Int. Ed.*, 2022, **61**, e20220688.
22 S. Tang, H. Ruan, Z. Hu, Y. Zhao, Y. Song and X. Wang, A cationic sulfur-hydrocarbon triradical with an excited quartet state, *Chem. Commun.*, 2022, **58**, 1986–1989.
23 K. Awaga, T. Sugano and M. Kinoshita, Ferromagnetic intermolecular interaction in the galvinoxyl radical: Cooperation of spin polarization and charge-transfer interaction, *Chem. Phys. Lett.*, 1987, **141**, 540–544.
24 S. Kasemthaveechok, L. Abella, J. Crassous, J. Autschbach and L. Favereau, Organic radicals with inversion of SOMO and HOMO energies and potential applications in optoelectronics, *Chem. Sci.*, 2022, **13**, 9833–9847.
25 N. C. Yang and A. J. Castro, Synthesis of a stable biradical, *J. Am. Chem. Soc.*, 1960, **82**, 6208.
26 K. Hinrichs, B. kirste, H. Kurreck and J. Reusch, Über galvinole und galvinoxyle—IV: Untersuchung dynamischer effekte an galvinoxyl-dublett-radikalen mit endor-in-lösung, *Tetrahedron*, 1977, **33**, 151–154.
27 B. Kirste, M. Grimm and H. Kurreck, EPR, proton and carbon-13 ENDOR studies of a quintet state 13C-labeled galvinoxyl-type tetraradical, *J. Am. Chem. Soc.*, 1989, **111**, 108–114.
28 D. A. Shultz and A. K. Boal, Nitroxyl-Galvinoxyl – A New Biradical, *Mol. Cryst. Liq. Cryst.*, 1995, **272**, 75–79.
29 D. A. Shultz and Q. Zhao, Preparation and characterization of a bis-galvinoxyl-disulfide, *Tetrahedron Lett.*, 1996, **37**, 8837–8840.
30 K. K. Anderson, D. A. Shultz and D. A. Dougherty, Attempted Synthesis of a Stable, Quintet, Tetraphenoxyl Tetraradical: Facile Rearrangement of a Substituted Bicyclobutane, *J. Org. Chem.*, 1997, **62**, 7575–7584.
31 M. Miyashita, T. Yamazaki and H. Nishide, Poly(3-phenylgalvinoxylthiophene). A New Conjugated Polyradical with High Spin Concentration, *Polym. J.*, 2001, **33**, 849–856.
32 P. Wautelet, P. Turek and J. Le Moigne, Synthesis of Phenyl Ethynylene Coupled Biradicals and Polyradicals Based on Galvinoxyl, *Synthesis*, 2002, 1286–1292.
33 E. Fukuzaki, N. Takahashi, S. Imai, H. Nishide and A. Rajca, Synthesis of Dendritic, Non-Kekulé-, and Nondisjoint-type Triphenylmethanes Terminated with Galvinoxyl Radicals, *Polym. J.*, 2005, **37**, 284–293.
34 T. Kaneko, H. Karagiri, Y. Umeda, T. Namikoshi, E. Marwanta, M. Teraguchi and T. Aoki, Optically active helical structure and magnetic interaction of poly(phenylacetylene)-based polyradicals, *Polyhedron*, 2009, **28**, 1927–1929.
35 T. Jähnert, B. Häupler, T. Janoschka, M. D. Hager and U. S. Schubert, Synthesis and Charge–Discharge Studies of Poly(ethynylphenyl)galvinoxyles and Their Use in Organic Radical Batteries with Aqueous Electrolytes, *Macromol. Chem. Phys.*, 2013, **214**, 2616–2623.
36 T. Chi, S. Akkiraju, Z. Liang, Y. Tan, H. J. Kim, X. Zhao, B. M. Savoie and B. W. Boudouris, Design of an n-type low glass transition temperature radical polymer, *Polym. Chem.*, 2021, **12**, 1448–1457.
37 S. Nakazono, S. Karasawa, N. Koga and H. Iwamura, Stabilization of p-Phenylenebis(N-tert-butylaminoxyl) Relative to p-Benzoquinonediimine N,N′-Dioxide, *Angew. Chem., Int. Ed.*, 1998, **37**, 1550–1552.
38 B. Kirste, W. Harrer, H. Kurreck, S. H. Bauer and W. Gierke, Hydrogen-1 and carbon-13 ENDOR investigations of sterically hindered galvinoxyl radicals, *J. Am. Chem. Soc.*, 1981, **103**, 6280–6286.

39 J. von Gersdorff, B. Kirste, D. Niethammer, W. Harrer and H. Kurreck, EPR and ENDOR investigations of dynamic processes in sterically overcrowded phenoxyl-type galvinoxyl radicals, *Magn. Reson. Chem.*, 1988, **26**, 416–424.

40 S. Stoll and A. Schweiger, EasySpin, a comprehensive software package for spectral simulation and analysis in EPR, *J. Magn. Reson.*, 2006, **178**, 42–55.

41 C. Hirel, K. E. Vostrikova, J. Pécaut, V. I. Ovcharenko and P. Rey, Nitronyl and Imino Nitroxides: Improvement of Ullman's Procedure and Report on a New Efficient Synthetic Route, *Chem. – Eur. J.*, 2001, **7**, 2007–2014.

42 J. K. Bjernemose and A. D. Bond, N,N-Bis[2-(2-pyridyl) ethyl]hydroxylamine, *Acta Crystallogr., Sect. E: Struct. Rep. Online*, 2004, **60**, o1143.

43 J. R. Malpass, P. S. Skerry and S. L. Rimmington, Meisenheimer and Other Rearrangements of N-Oxides Derived from 2-Azabicyclo[2.2.1]hept-5-enes; the Influence of Reaction Conditions and Stereochemistry at Nitrogen, *Heterocycles*, 2004, **62**, 679–691.

44 C. Berini, F. Minassian, N. Pelloux-Léon, J.-N. Denis, Y. Vallée and C. Philouze, Efficient stereoselective nucleophilic addition of pyrroles to chiral nitrones, *Org. Biomol. Chem.*, 2008, **6**, 2574–2586.

45 A. Okazawa, Y. Nagaichi, T. Nogami and T. Ishida, Magneto-Structure Relationship in Copper(II) and Nickel(II) Complexes Chelated with Stable tert-Butyl 5-Phenyl-2-pyridyl Nitroxide and Related Radicals, *Inorg. Chem.*, 2008, **47**, 8859–8868.

46 P. A. Tziouris, C. G. Tsiafoulis, M. Vlasiou, H. N. Miras, M. P. Sigalas, A. D. Keramidas and T. A. Kabanos, Interaction of Chromium(III) with a N,N′-Disubstituted Hydroxylamine-(diamido) Ligand: A Combined Experimental and Theoretical Study, *Inorg. Chem.*, 2014, **53**, 11404–11414.

47 I. Golomolzina, S. Tolstikov, G. Letyagin, G. Romanenko, A. S. Bogomyakov, A. Y. Akyeva, M. A. Syroeshkin, M. P. Egorov, V. Morozov and V. Ovcharenko, Cu(hfac)$_2$ Complexes with Acyclic Nitroxide Prone to Single-Crystal to Single-Crystal Transformation and Showing Mechanical Activity, *Cryst. Growth Des.*, 2022, **22**, 6148–6167.

48 A. M. Lobo, S. Prabhakar, H. S. Rzepa, A. C. Skapski, M. R. Tavares and D. A. Widdowson, C-substitution reactions of c,n-diaryl nitrones, *Tetrahedron*, 1983, **39**, 3833–3841.

49 J.-G. Kang, J.-P. Hong and I.-H. Suh, N,-(4-Cyanophenyl)-α-(4-methoxyphenyl)nitrone, *Acta Crystallogr., Sect. C: Cryst. Struct. Commun.*, 2000, **56**, 231–232.

50 R. Herrera, A. Nagarajan, M. A. Morales, F. Méndez, H. A. Jiménez-Vázquez, L. G. Zepeda and J. Tamariz, Regio- and Stereoselectivity of Captodative Olefins in 1,3-Dipolar Cycloadditions. A DFT/HSAB Theory Rationale for the Observed Regiochemistry of Nitrones, *J. Org. Chem.*, 2001, **66**, 1252–1263.

51 H. Hopf, A. A. Aly, V. N. Swaminathan, L. Ernst, I. Dix and P. G. Jones, A Simple Route to a Pyridinyl[2.2]paracyclophane, *Eur. J. Org. Chem.*, 2005, 68–71.

52 C. Riplinger, J. P. Y. Kao, G. M. Rosen, V. Kathirvelu, G. R. Eaton, S. S. Eaton, A. Kutateladze and F. Neese, Interaction of Radical Pairs Through-Bond and Through-Space: Scope and Limitations of the Point–Dipole Approximation in Electron Paramagnetic Resonance Spectroscopy, *J. Am. Chem. Soc.*, 2009, **131**, 10092–10106.

53 W. Frey, A. Baskakova, A. Menzel and V. Jäger, Crystal structure of 2,3-O-cyclohexylidene-D-glyceraldehyde N-benzylnitrone, $C_{16}H_{21}NO_3$, *Z. Kristallogr. - New Cryst. Struct.*, 2010, **225**, 245–246.

54 M. Tanaka, K. Matsuda, T. Itoh and H. Iwamura, Syntheses and Magnetic Properties of Stable Organic Triradicals with Quartet Ground States Consisting of Different Nitroxide Radicals, *J. Am. Chem. Soc.*, 1998, **120**, 7168–7173.

55 Y. Hosokoshi, K. Katoh, Y. Nakazawa, H. Nakano and K. Inoue, Approach to a Single-Component Ferrimagnetism by Organic Radical Crystals, *J. Am. Chem. Soc.*, 2001, **123**, 7921–7922.

56 T. Itoh, K. Matsuda, H. Iwamura and K. Hori, The Ground Spin States of Tris[p-(N-oxyl-N-tert-butylamino)phenyl] amine, -Methyl, and -Borane. Prospects of Further Studies, *J. Solid State Commun.*, 2001, **159**, 428–439.

57 J. Ohshita, T. Iida, N. Ohta, K. Komaguchi, M. Shiotani and A. Kunai, Synthesis of Phenylnitroxides Bridged by an sp^3-Linkage, *Org. Lett.*, 2002, **4**, 403–406.

58 D. A. Shultz, R. M. Fico Jr., H. Lee, J. W. Kampf, K. Kirschbaum, A. A. Pinkerton and P. D. Boyle, Mechanisms of Exchange Modulation in Trimethylenemethane-type Biradicals: The Roles of Conformation and Spin Density, *J. Am. Chem. Soc.*, 2003, **125**, 15426–15432.

59 G. Kurokawa, T. Ishida and T. Nogami, Remarkably strong intermolecular antiferromagnetic couplings in the crystal of biphenyl-3,5-diyl bis(tert-butyl nitroxide), *Chem. Phys. Lett.*, 2004, **392**, 74–79.

60 O. B. Borobia, P. Guionneau, H. Heise, F. H. Köhler, L. Ducasse, J. Vidal-Gancedo, J. Veciana, S. Golhen, L. Ouahab and J.-P. Sutter, Discrepancy between the Spin Distribution and the Magnetic Ground State for a Triaminoxyl Substituted Triphenylphosphine Oxide Derivative, *Chem. – Eur. J.*, 2005, **11**, 128–139.

61 Z. Delen and P. M. Lahti, Crystallography and Magnetism of Two 1-(4-Nitroxylphenyl)pyrroles, *J. Org. Chem.*, 2006, **71**, 9341–9347.

62 H. Nishimaki, S. Mashiyama, M. Yasui, T. Nogami and T. Ishida, Bistable Polymorphs Showing Diamagnetic and Paramagnetic States of an Organic Crystalline Biradical Biphenyl-3,5-diyl Bis(tert-butylnitroxide), *Chem. Mater.*, 2006, **18**, 3602–3604.

63 N. Roques, P. Gerbier, U. Schatzschneider, J.-P. Sutter, P. Guionneau, J. Vidal-Gancedo, J. Veciana, E. Rentschler and C. Guérin, Experimental and Theoretical Studies of Magnetic Exchange in Silole-Bridged Diradicals, *Chem. – Eur. J.*, 2006, **12**, 5547–5562.

64 H. Nishimaki and T. Ishida, Organic Two-Step Spin-Transition-Like Behavior in a Linear S = 1 Array: 3′-

Methylbiphenyl-3,5-diyl Bis(tert-butylnitroxide) and Related Compounds, *J. Am. Chem. Soc.*, 2010, **132**, 9598–9599.

65 T. Konno, H. Kudo and T. Ishida, Intermediate-paramagnetic phases with a half and a quarter spin entities in fluorinated biphenyl-3,5-diyl bis(tert-butyl nitroxides), *J. Mater. Chem. C*, 2015, **3**, 7813–7918.

66 H. Kawakami, A. Tonegawa and T. Ishida, Pyridine-2,6-diyl dinitroxides as room-temperature triplet ligands, *AIP Conf. Proc.*, 2016, **1709**, 020017.

67 H. Kawakami, A. Tonegawa and T. Ishida, A designed room-temperature triplet ligand from pyridine-2,6-diyl bis (tert-butyl nitroxide), *Dalton Trans.*, 2016, **45**, 1306–1309.

68 T. Yoshitake, H. Kudo and T. Ishida, Thermally Activated Paramagnets from Diamagnetic Polymers of Biphenyl-3,5-diyl Bis(tert-butyl Nitroxides) Carrying Methyl and Fluoro Groups at the 2′- and 5′-Positions, *Crystals*, 2016, **6**, 30.

69 N. Koizumi and T. Ishida, Forced proximity of nitroxide groups in pincer compounds with a xanthene spacer, *Tetrahedron Lett.*, 2017, **58**, 2804–2808.

70 A. Okazawa, Y. Terakado, T. Ishida and N. Kojima, A triplet biradical with double bidentate sites based on tert-butyl pyridyl nitroxide as a candidate for strong ferromagnetic couplers, *New J. Chem.*, 2018, **42**, 17874–17878.

71 H. Han, D. Zhang, Z. Zhu, R. Wei, X. Xiao, X. Wang, Y. Liu, Y. Ma and D. Zhao, Aromatic Stacking Mediated Spin–Spin Coupling in Cyclophane-Assembled Diradicals, *J. Am. Chem. Soc.*, 2021, **143**, 17690–17700.

72 M. Nakagawa, T. Ishida, M. Suzuki, D. Hashizume, M. Yasui, F. Iwasaki and T. Nogami, Intermolecular ferromagnetic interaction in the crystal of a diphenyl nitroxide derivative. The role of spin-polarized hydrogen atoms located near a neighboring N–O site, *Chem. Phys. Lett.*, 1999, **302**, 125–131.

73 T. Ishida, M. Ooishi, N. Ishii, H. Mori and T. Nogami, Mono- and dinitroxide radicals from 9,9′(10H,10′H)-spirobiacridine: An approach to a D2d triplet biradical, *Polyhedron*, 2007, **26**, 1793–1799.

74 T. Kanetomo, K. Ichihashi, M. Enomoto and T. Ishida, Ground Triplet Spirobiradical: 2,2′,7,7′-Tetra(tert-butyl)-9,9′(10H,10′H)-spirobiacridine-10,10′-dioxyl, *Org. Lett.*, 2019, **21**, 3909–3912.

75 K. Ichihashi, T. Kanetomo, M. Enomoto and T. Ishida, 2,7-Di-tert-butyl-9,9′(10H,10′H)-spirobiacridine-10,10′-dioxyl as a ground triplet biradical: The role of tert-butylation, *Tetrahedron Lett.*, 2020, **61**, 152428.

76 A. Zheludev, V. Berone, M. Bonnet, B. Delley, A. Grand, E. Ressouche, P. Rey, R. Subra and J. Schweizer, Spin density in a nitronyl nitroxide free radical. Polarized neutron diffraction investigation and ab initio calculations, *J. Am. Chem. Soc.*, 1994, **116**, 2019–2027.

77 M. M. Matsushita, A. Izuoka, T. Sugawara, T. Kobayashi, N. Wada, N. Takeda and M. Ishikawa, Hydrogen-Bonded Organic Ferromagnet, *J. Am. Chem. Soc.*, 1997, **119**, 4369–4379.

78 R. Akabane, M. Tanaka, K. Matsuo, N. Koga, K. Matsuda and H. Iwamura, Crystal Structures and Magnetic Properties of m-Phenylenebis(imidazole) Derivatives Having Two Nitronyl Nitroxide or Iminyl Nitroxide Radicals. The Two Kinds of Antiferromagnetic Interaction Alternating along One-Dimensional Chains, *J. Org. Chem.*, 1997, **62**, 8854–8861.

79 N. L. Frank, R. Clérac, J.-P. Sutter, N. Daro, O. Kahn, C. Coulon, M. T. Green, S. Golhen and L. Ouahab, Synthesis, Crystal Structure, Magnetic, and Electron Paramagnetic Resonance Properties of a Spiroconjugated Biradical. Evidence for Spiroconjugation Exchange Pathway, *J. Am. Chem. Soc.*, 2000, **122**, 2053–2061.

80 J. Nakazaki, I. Chung, M. M. Matsushita, T. Sugawara, R. Watanabe, A. Izuoka and Y. Kawada, Design and preparation of pyrrole-based spin-polarized donors, *J. Mater. Chem.*, 2003, **13**, 1011–1022.

81 P. Brough, R. Chiarelli, J. Pécaut, A. Rassat and P. Rey, A versatile synthesis of new pyrimidinyl nitronyl nitroxides, *Chem. Commun.*, 2003, 2722–2723.

82 Y. Masuda, M. Kuratasu, S. Suzuki, M. Kozaki, D. Shiomi, K. Sato, T. Takui, Y. Hosokoshi, X.-Z. Lan, Y. Miyazaki, A. Inaba and K. Okada, A New Ferrimagnet Based on a Radical-Substituted Radical Cation Salt, *J. Am. Chem. Soc.*, 2009, **131**, 4670–4673.

83 K. Kolanji, L. Postulka, B. Wolf, M. Lang, D. Schollmeyer and M. Baumgarten, Planar Benzo[1,2-b:4,5-b′]dithiophene Derivatives Decorated with Nitronyl and Imino Nitroxides, *J. Org. Chem.*, 2019, **84**, 140–149.

84 E. V. Tretyakov, P. V. Petunin, S. I. Zhivetyeva, D. E. Gorbunov, N. P. Gritsan, M. V. Fedin, D. V. Stass, R. I. Samoilova, I. Y. Bagryanskaya, I. K. Shundrina, A. S. Bogomyakov, M. S. Kazantsev, P. S. Postnikov, M. E. Trusova and V. I. Ovcharenko, Platform for High-Spin Molecules: A Verdazyl-Nitronyl Nitroxide Triradical with Quartet Ground State, *J. Am. Chem. Soc.*, 2021, **143**, 8164–8176.

85 C. Shu, M. Pink, T. Junghoefer, E. Nadler, S. Rajca, M. B. Casu and A. Rajca, Synthesis and Thin Films of Thermally Robust Quartet (S = 3/2) Ground State Triradical, *J. Am. Chem. Soc.*, 2021, **143**, 5508–5518.

86 P. Ravat and M. Baumgarten, "Tschitschibabin type biradicals": benzenoid or quinoid?, *Phys. Chem. Chem. Phys.*, 2015, **17**, 983–991.

87 J. Kruszewski and T. M. Krygowski, Definition of aromaticity basing on the harmonic oscillator model, *Tetrahedron Lett.*, 1972, **13**, 3839–3842.

88 T. M. Krygowski, Crystallographic studies of inter- and intramolecular interactions reflected in aromatic character of .pi.-electron systems, *J. Chem. Inf. Comput. Sci.*, 1993, **33**, 70–78.

89 A. Bondi, van der Waals Volumes and Radii, *J. Phys. Chem.*, 1964, **68**, 441–451.

90 O. Kahn, *Molecular Magnetism*, VCH-Verlag, Weinheim, New York, 1993.

91 T. Onishi, D. Yamaki, K. Yamaguchi and Y. Takano, Theoretical calculations of effective exchange integrals by spin projected and unprojected broken-symmetry methods. I. Cluster models of K_2NiF_4-type solids, *J. Chem. Phys.*, 2003, **118**, 9747–9761.

